Hydrogeochemical Evolution and Drinking Water Suitability Assessment of Groundwater in Semi-Arid Basaltic Terrain of Akkalkot Taluka, Maharashtra, India

Mustaq Shaikh[1*], Farjana Birajdar[2]

[1]Senior Geologist, Groundwater Surveys and Development Agency, Solapur, Maharashtra, India

[2]Assistant Geologist, Groundwater Surveys and Development Agency, Solapur, Maharashtra, India

DOI: https://doi.org/10.51244/IJRSI.2026.1305000253

Received: 24 May 2026; Accepted: 30 May 2026; Published: 12 June 2026

ABSTRACT

Groundwater is the principal source of drinking and irrigation water in the semi-arid Deccan basaltic terrain of Akkalkot taluka, Solapur district, Maharashtra. This study assesses the hydrogeochemical evolution, the geochemical processes governing groundwater composition, and the drinking-water suitability of the resource using 5,352 groundwater samples drawn from handpumps, dug wells and borewells over eight hydrological years (2016–17 to 2023–24). The water is neutral to slightly alkaline (mean pH 7.5) and predominantly hard to very hard (93% exceed 150 mg L^{-1} as $CaCO_3$). Electrical conductivity (mean 1,532 µS cm^{-1}) and total dissolved solids (mean 989 mg L^{-1}) indicate moderate mineralization. Piper and Chadha diagrams reveal a mixed facies assemblage dominated by Ca–Mg–HCO_3 recharge water (33%) that evolves towards Na–HCO_3 and Na–Cl types. Gibbs plots, Na^+/Cl^- ratios (>1 in 74% of samples) and negative chloro-alkaline indices (74%) identify silicate (plagioclase) weathering and cation exchange as the dominant controls, modified by evapoconcentration. Elevated nitrate (exceeding the 45 mg L^{-1} limit in 29% of samples) reflects anthropogenic loading from both agricultural fertilizers and sanitation sources. The weighted-arithmetic water quality index rated 78% of samples as excellent–good; hardness, salinity and nitrate are the chief constraints on potability.

Keywords: Hydrogeochemistry; Deccan basalt; Piper diagram; Hydrochemical facies; Water–rock interaction; Water Quality Index; Drinking water suitability.

INTRODUCTION

Groundwater sustains domestic supply, irrigation and rural livelihoods across the basaltic uplands of peninsular India, where surface water is seasonal and unevenly distributed (K.R. Karanth, 1987). The Deccan Volcanic Province, one of the largest continental flood-basalt provinces on Earth, forms a complex, multi-layered hard-rock aquifer system in which groundwater occurs chiefly in the weathered mantle, vesicular horizons and interconnected fracture networks of successive lava flows (P.K. Naik, 2003). Because storage and circulation are confined to these shallow, heterogeneous zones, basaltic groundwater is highly responsive to recharge, residence time and human activity, and its chemistry records the cumulative imprint of water–rock interaction (N.J. Pawar, 1998).

In semi-arid settings, high evaporation, prolonged rock contact and intensifying agricultural and domestic stress frequently degrade groundwater quality through rising salinity, hardness, nitrate and, locally, fluoride (N. Subba Rao, 2006; N. Adimalla, 2018; V.M. Wagh, 2019). Characterizing the hydrogeochemistry of such aquifers is therefore essential both for understanding the natural evolution of groundwater and for safeguarding public health (M.A. Shaikh, 2024a). Graphical and ratio-based diagnostics—the Piper trilinear diagram (A.M. Piper, 1944), the Chadha rectangular diagram (D.K. Chadha, 1999), the Gibbs boomerang (R.J. Gibbs, 1970) and the Schoeller chloro-alkaline indices (H. Schoeller, 1965)—remain powerful tools for resolving hydrochemical facies and the processes that generate them. Suitability for human consumption is judged against national and international specifications (BIS, 2012; WHO, 2017) and synthesized through the water quality index (M. Vasanthavigar, 2010).

ISSN No. 2321-2705 | DOI: 10.51244/IJRSI |Volume XIII Issue V May 2026

Despite extensive work on Deccan basalt groundwater elsewhere in Maharashtra (D. Marghade, 2012; D.B. Panaskar, 2016; V.M. Wagh, 2019), the Akkalkot taluka of Solapur district—a drought-prone, intensively cultivated basaltic tract along the Maharashtra–Karnataka border—has received little systematic hydrogeochemical attention (M. Shaikh., 2025). The present study addresses this gap using a large, multi-year regulatory monitoring dataset. The specific objectives are: (i) to characterize the major-ion chemistry and hydrochemical facies of the groundwater; (ii) to identify the water–rock interaction and other processes controlling its composition; (iii) to examine seasonal and inter-annual chemical evolution; and (iv) to evaluate drinking- and irrigation-water suitability against BIS and WHO standards.

Study Area

Location and physiography

Akkalkot taluka occupies the south-eastern corner of Solapur district in south Maharashtra, lying approximately between 17°15′ and 17°45′ N latitude and 76°00′ and 76°35′ E longitude, and bordering Karnataka to the south and east (Figure 1). The terrain is a gently undulating basaltic plateau with subdued relief, drained by minor tributaries of the Bhima River sub-basin. Agriculture—predominantly sugarcane, pulses, sorghum and oilseeds—is the dominant land use and the main consumer of groundwater (F. Birajdar, 2024d).

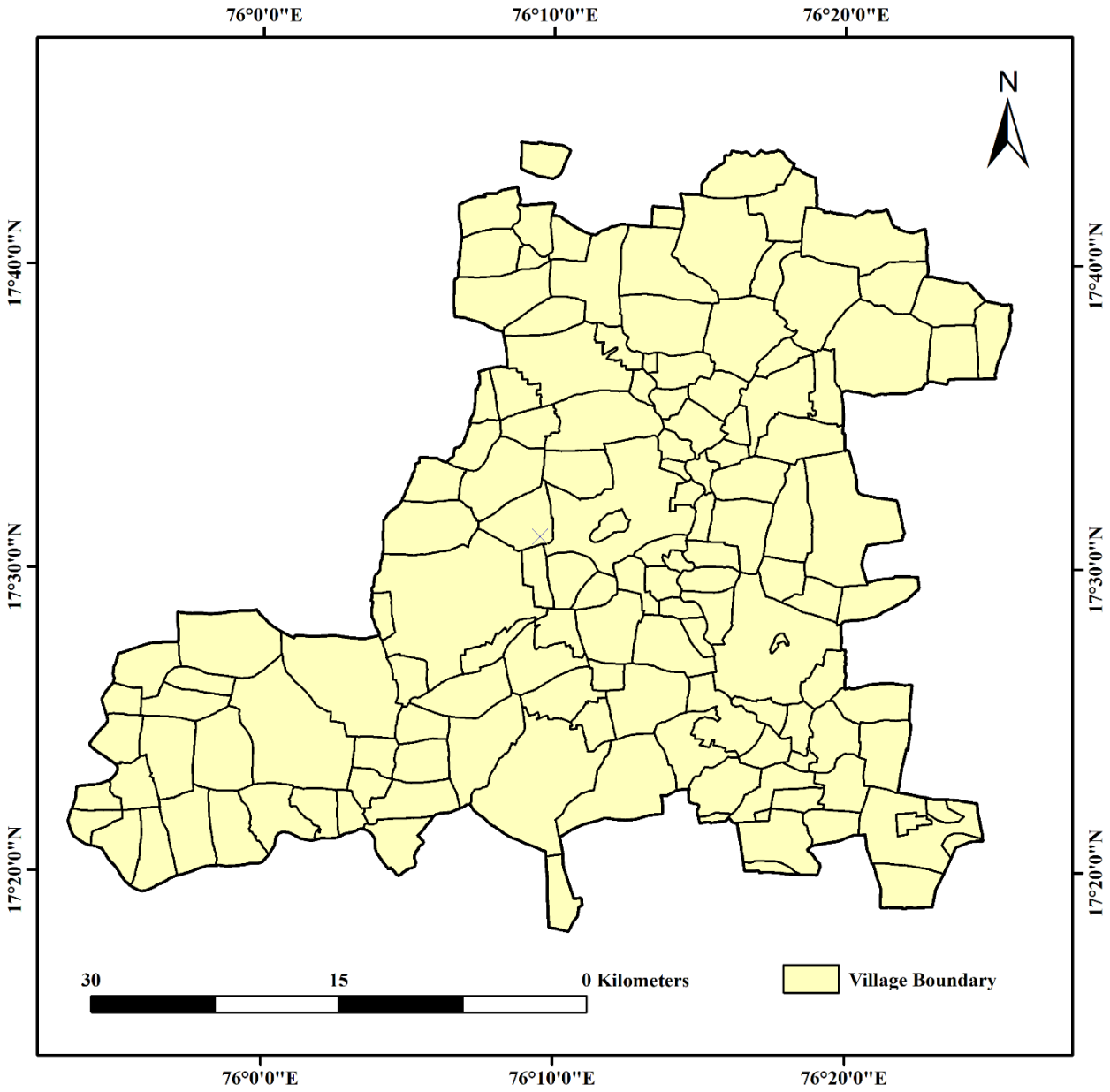

Figure 1. Location of the study area

ISSN No. 2321-2705 | DOI: 10.51244/IJRSI |Volume XIII Issue V May 2026

Climate and drainage

The area experiences a semi-arid climate with three distinct seasons: a hot pre-monsoon summer (March–May), a south-west monsoon (June–September) and a cool post-monsoon–winter period (October–February). Mean annual rainfall is modest (approximately 650–750 mm) and largely confined to the monsoon, while potential evapotranspiration is high, producing a pronounced moisture deficit for much of the year (CGWB, 2013). Drainage is dendritic and ephemeral, so rainfall recharge to the shallow aquifer is brief and episodic, favouring evaporative concentration of dissolved salts during the long dry season.

Geology and hydrogeology

The taluka is underlain entirely by sub-horizontal basaltic lava flows of the Deccan Trap (Upper Cretaceous–Palaeocene), composed of alternating massive (compact) and vesicular/amygdaloidal flow units with intervening weathered, jointed and fractured zones (P.K. Naik, 2003). The basalts are tholeiitic, rich in calcic plagioclase (labradorite–andesine), clinopyroxene (augite) and volcanic glass, with secondary zeolites, calcite and clay minerals filling vesicles—mineral assemblages that strongly influence the dissolved-ion chemistry. Groundwater occurs under water-table to semi-confined conditions within the weathered mantle and vesicular–fractured horizons, which together constitute a shallow, low-to-moderate yielding aquifer system, while the massive flow interiors act as local aquicludes (Figure 2). Recharge is chiefly from direct monsoon infiltration; discharge is through wells, springs and evapotranspiration.

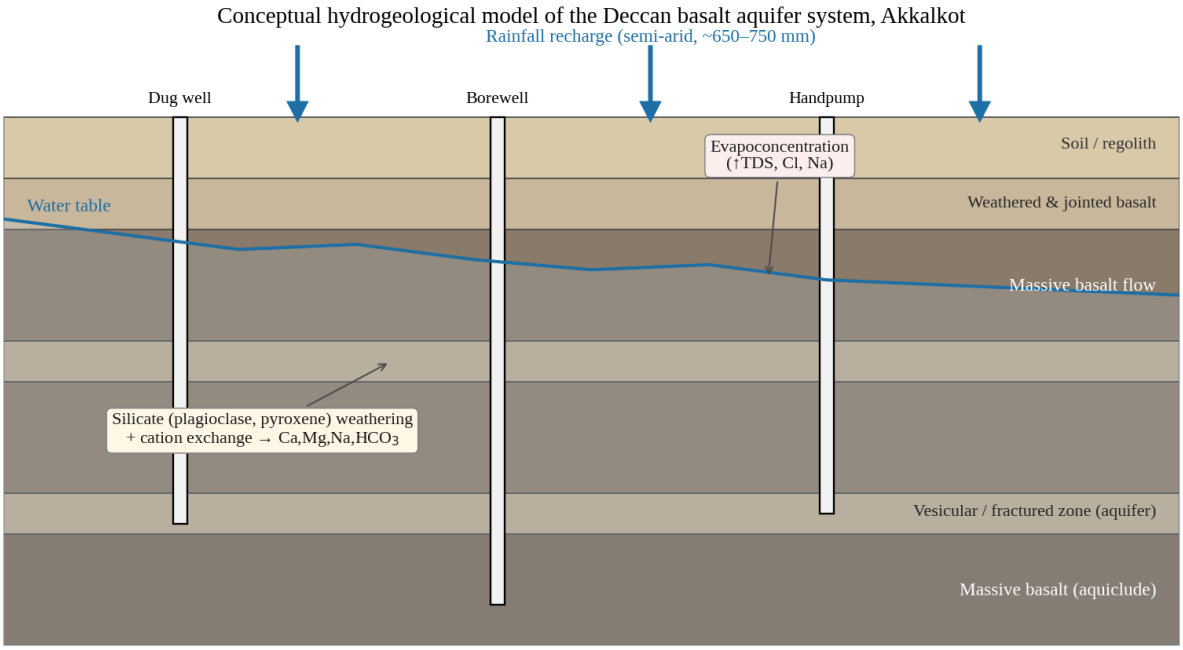

Figure 2. Conceptual hydrogeological model of the Deccan basalt aquifer system at Akkalkot, showing alternating massive and vesicular/fractured flow units, the weathered zone, water table, principal abstraction structures, and the dominant geochemical processes.

MATERIALS AND METHODS

Data source and sampling

Groundwater quality data were obtained from the routine Water Quality Monitoring and Surveillance Programme operated by the district and sub-divisional public-health laboratories of the Government of Maharashtra, which periodically test village drinking-water sources (M.A. Shaikh, 2024c). From the state archive, all records pertaining to Akkalkot taluka for eight hydrological years (2016–17 to 2023–24) were extracted, yielding 6,067 entries. To restrict the analysis to groundwater, samples from surface and distribution sources (storage tanks, reservoirs, taps and stand-posts) were removed; the retained dataset comprises 5,352 samples from handpumps (42%), dug wells (30%) and borewells (28%) distributed across the taluka.

ISSN No. 2321-2705 | DOI: 10.51244/IJRSI |Volume XIII Issue V May 2026

Each sample was analysed for pH, electrical conductivity (EC), total dissolved solids (TDS), total alkalinity, total hardness (TH), chloride (Cl^-), sulphate (SO_4^{2-}), nitrate (NO_3^-), fluoride (F^-) and iron (Fe) following standard procedures (APHA, 2017): pH and EC by electrode and conductivity meter; TDS gravimetrically/by EC conversion; alkalinity and hardness by acid and EDTA titration, respectively; chloride by the argentometric method; sulphate turbidimetrically; nitrate and fluoride by spectrophotometry and ion-selective electrode; and iron by the phenanthroline method. As is typical of regulatory surveillance datasets, calcium and magnesium were not reported individually and sodium and potassium were not determined; the treatment of these species is detailed in Section 3.2. Concentrations are reported in mg L^{-1} (1 mg $L^{-1} \approx 1$ g m^{-3} in SI units) and EC in µS cm^{-1}.

Derived ionic concentrations and charge balance

All concentrations were converted to milli-equivalents per litre (meq L^{-1}) using standard equivalent weights (J.D. Hem, 1985). Combined alkaline-earth concentration ($Ca^{2+} + Mg^{2+}$) was derived from total hardness expressed as $CaCO_3$, and bicarbonate (HCO_3^-) from total alkalinity, which is justified by the observed pH range (5.9–9.4, mean 7.5) in which bicarbonate is the dominant alkalinity species. Because Na^+ and K^+ were not measured, the combined alkali concentration ($Na^+ + K^+$) was estimated by ionic charge-balance closure:

$$(Na^+ + K^+) = \Sigma \text{ anions} - (Ca^{2+} + Mg^{2+}) \quad [\text{meq } L^{-1}], \quad \Sigma \text{ anions} = HCO_3^- + Cl^- + SO_4^{2-} + NO_3^- + F^-$$

This widely used approximation forces electroneutrality and assumes a negligible contribution from unmeasured species. The 3.1% of samples returning a physically implausible negative residual—indicative of analytical inconsistency in the reported hardness or alkalinity—were excluded from facies classification (final facies n = 5,188). For the Piper cation triangle only, total hardness was apportioned into Ca^{2+} and Mg^{2+} using a TDS-dependent molar Ca/Mg ratio (≈ 1.7 in dilute recharge water decreasing to ≈ 0.7 at high salinity), consistent with progressive magnesium enrichment during calcite precipitation reported for Deccan basalt aquifers (N.J. Pawar, 1998, M.A. Shaikh 2024). It is emphasized that the Piper diamond and the Chadha diagram—on which facies assignment is based—are mathematically independent of this Ca/Mg split; the cation-triangle positions are therefore indicative only, whereas the facies classification is robust. To illustrate the sensitivity of cation-triangle positions to this assumption, Appendix A presents the Piper diagram reproduced under two end-member Ca/Mg ratios (fixed at 1.7 and 0.7 throughout), demonstrating that facies boundaries in the central diamond are unaffected. The full rationale for the TDS-dependent splitting function, together with the range of calculated Ca^{2+}, Mg^{2+} and Na^++K^+ values and their charge-balance uncertainty bounds, is provided in Appendix A to keep the main text focused on interpretive results.

Geochemical diagnostics

Hydrochemical facies were resolved using the Piper trilinear diagram (A.M. Piper, 1944) and the Chadha rectangular diagram (D.K. Chadha, 1999). The processes controlling solute acquisition were investigated with the Gibbs diagrams (R.J. Gibbs, 1970), the Na^+/Cl^- ratio, the $(Ca^{2+} + Mg^{2+})/(HCO_3^- + SO_4^{2-})$ and $(Ca^{2+} + Mg^{2+})/HCO_3^-$ ratios, and the Schoeller chloro-alkaline indices CAI-I and CAI-II (H. Schoeller, 1965), which diagnose the direction of cation exchange.

Suitability indices

Drinking-water suitability was assessed against the Indian Standard IS 10500:2012 (BIS, 2012) and the WHO guidelines (WHO, 2017), and synthesized through the weighted-arithmetic water quality index (WQI) of M. Vasanthavigar (2010). Each parameter was assigned a weight reflecting its relative health significance (NO_3^- and F^- = 5; pH, TDS, SO_4^{2-} and Fe = 4; alkalinity and Cl^- = 3; TH = 2); relative weights were computed, the quality rating $q_i = (C_i/S_i) \times 100$ (with the ideal value of pH taken as 7), and $WQI = \Sigma(w_i\, q_i)$. Irrigation suitability was evaluated using the sodium adsorption ratio (SAR; L.A. Richards, 1954), sodium percentage (Na%; after L.V. Wilcox, 1955), residual sodium carbonate (RSC; F.M. Eaton, 1950), Kelley's ratio (W.P. Kelley, 1940) and the permeability index (PI; L.D. Doneen, 1964). Hardness classes follow C.N. Sawyer and P.L. McCarty (1967).

ISSN No. 2321-2705 | DOI: 10.51244/IJRSI |Volume XIII Issue V May 2026

Statistical analysis

Descriptive statistics (minimum, maximum, mean, standard deviation, median) and the Pearson product-moment correlation matrix were computed for all parameters using standard methods (APHA, 2017). Data handling, statistical computation and graphical construction were performed in Python (pandas and Matplotlib libraries). Samples were grouped by season—pre-monsoon (March–May), monsoon (June–September) and post-monsoon (October–February)—to examine seasonal evolution.

RESULTS AND DISCUSSION

General hydrochemistry and major-ion chemistry

Summary statistics for the 5,352 groundwater samples, together with BIS and WHO specifications, are presented in Table 1, and the distribution of key parameters is shown in Figure 3. The groundwater is neutral to slightly alkaline (pH 5.9–9.4, mean 7.5), consistent with a bicarbonate-buffered system dominated by silicate hydrolysis. Electrical conductivity ranges widely (mean 1,532 µS cm^{-1}; median 1,282 µS cm^{-1}) and TDS averages 989 mg L^{-1}, classifying most samples as moderately mineralized fresh water, although a minority are brackish. The wide spread reflects the heterogeneity of the basaltic aquifer and variable residence times.

Among anions, bicarbonate dominates (mean 341 mg L^{-1}), followed by chloride (mean 172 mg L^{-1}), sulphate (95 mg L^{-1}), nitrate (57 mg L^{-1}) and fluoride (0.2 mg L^{-1}), giving the general anion order $HCO_3^- > Cl^- > SO_4^{2-} > NO_3^- > F^-$. The alkaline earths ($Ca^{2+} + Mg^{2+}$, mean 379 mg L^{-1} as $CaCO_3$) and the derived alkalis ($Na^+ + K^+$) are the principal cations. The dominance of bicarbonate and alkaline earths, together with appreciable sodium, is the geochemical signature of silicate weathering in basalt, where the dissolution of calcic plagioclase and pyroxene releases Ca^{2+}, Mg^{2+}, Na^+ and HCO_3^- (N.J. Pawar, 1998; D. Marghade, 2012). Total hardness averages 379 mg L^{-1} as $CaCO_3$, and on the classification of C.N. Sawyer and P.L. McCarty (1967) 53% of samples are very hard and a further 41% hard—hardness being the single most pervasive quality concern in the area.

Table 1. Descriptive statistics of groundwater quality parameters at Akkalkot (n = 5,352) and comparison with BIS (2012) and WHO (2017) drinking-water standards. Parameters marked * are derived (see Section 3.2). Units in mg L^{-1} unless stated.

Parameter	Unit	Min	Max	Mean	SD	BIS acceptable	BIS permissible	WHO
pH	–	5.95	9.36	7.54	0.32	6.5–8.5	–	6.5–8.5
EC	µS cm^{-1}	0.14	9202.0	1531.8	822.72	–	–	–
TDS	mg L^{-1}	53.0	9692.0	988.58	544.13	500	2000	1000
Total alkalinity	mg L^{-1}	20.0	862.0	279.84	96.34	200	600	–
Total hardness	mg L^{-1}	1.2	2800.0	379.37	255.61	200	600	500
Bicarbonate (HCO3)	mg L^{-1}	24.39	1051.14	341.25	117.48	–	–	–
Calcium (Ca)*	mg L^{-1}	0.24	560.67	75.97	51.18	–	–	–
Magnesium (Mg)*	mg L^{-1}	0.15	339.93	46.06	31.03	–	–	–
Sodium+Potassium*	mg L^{-1}	-311.5	796.79	132.23	94.64	–	–	–
Chloride (Cl)	mg L^{-1}	8.0	1390.0	171.81	164.75	250	1000	250

ISSN No. 2321-2705 | DOI: 10.51244/IJRSI |Volume XIII Issue V May 2026

Sulphate (SO4)	mg L^{-1}	0.0	800.0	94.59	74.86	200	400	250
Nitrate (NO3)	mg L^{-1}	0.0	351.86	56.75	43.16	45	NR	50
Fluoride (F)	mg L^{-1}	0.0	2.4	0.2	0.22	1.0	1.5	1.5
Iron (Fe)	mg L^{-1}	0.0	1.1	0.05	0.06	0.3	NR	0.3
Turbidity	NTU	0.0	31.4	1.31	0.96	–	–	–

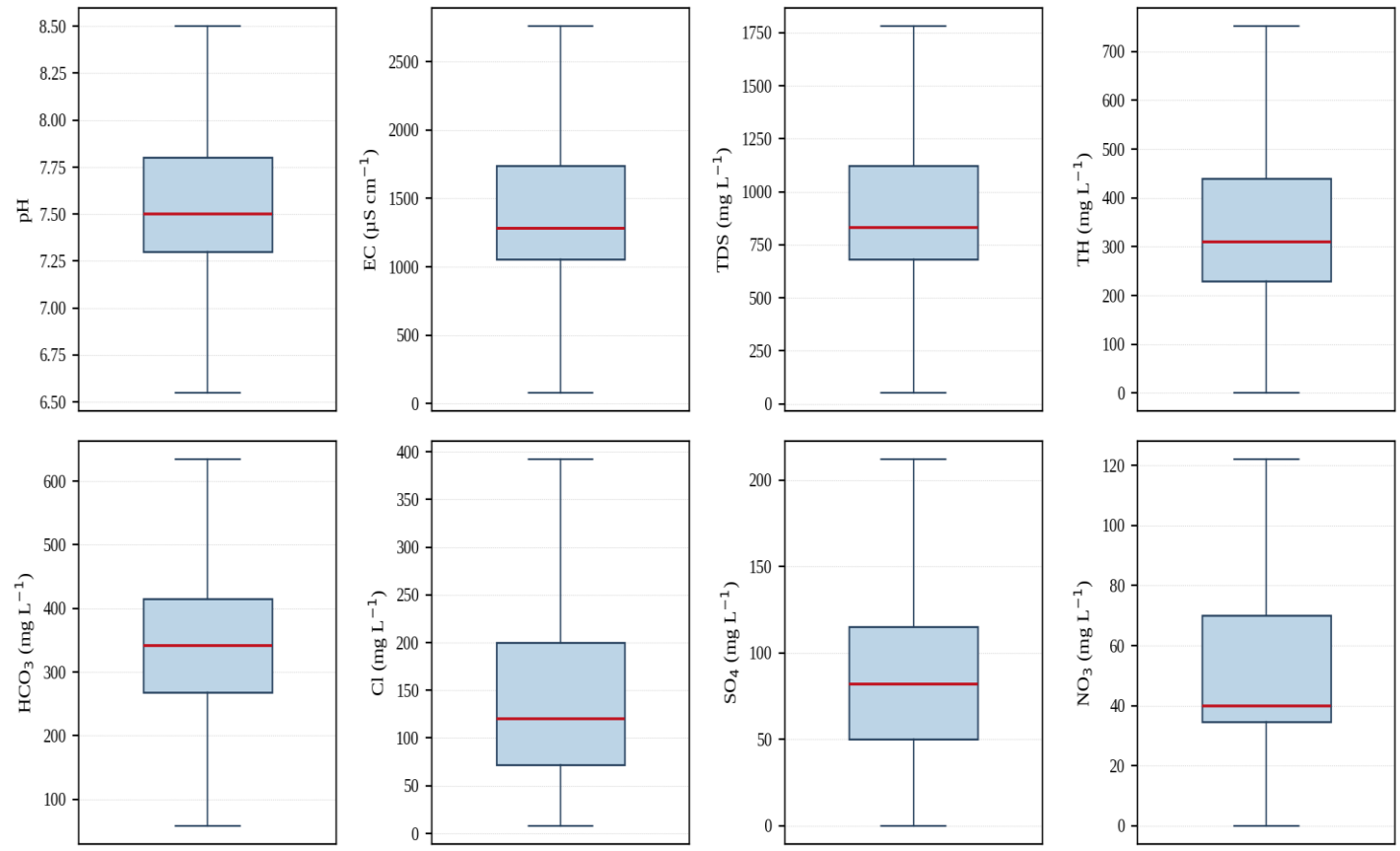

Figure 3. Box-and-whisker plots of major physico-chemical parameters of the Akkalkot groundwater (boxes = inter-quartile range; central line = median; whiskers = 1.5×IQR).

Hydrogeochemical facies

The Piper trilinear diagram (Figure 4) and the Chadha rectangular diagram (Figure 5) consistently reveal a mixed hydrochemical character rather than a single dominant facies. In the cation field the samples spread from the Ca–Mg corner towards the Na + K apex, recording progressive alkalization; in the anion field bicarbonate and chloride share dominance with subordinate sulphate. In the diagnostic Piper diamond, the alkaline-earth fields (Ca + Mg) account for 59% of samples and the alkali fields (Na + K) for 41%, while weak-acid (HCO_3) and strong-acid (Cl + SO_4) anions are nearly balanced. The resulting facies distribution (Table 2) is led by the Ca–Mg–HCO_3 type (33%), the hallmark of recently recharged, relatively fresh groundwater, followed by Ca–Mg–Cl/SO_4 (27%), Na–Cl (21%) and Na–HCO_3 (20%) types.

This assemblage describes a coherent evolutionary sequence: dilute Ca–Mg–HCO_3 recharge water acquires sodium and chloride during prolonged residence and evapoconcentration, migrating across the diamond towards Na–HCO_3 (via cation exchange) and ultimately Na–Cl (evolved/saline) compositions. The Chadha diagram (Figure 5) reinforces this interpretation, with a large population in the Ca–Mg–HCO_3 (recharging) field and a well-developed limb extending into the Na–HCO_3 (base-ion-exchange) and Na–Cl fields. Such mixed and

ISSN No. 2321-2705 | DOI: 10.51244/IJRSI |Volume XIII Issue V May 2026

evolving facies are characteristic of semi-arid Deccan basalt aquifers, where short flow paths, heterogeneous fracturing and intense evaporation operate together (D.B. Panaskar, 2016; V.M. Wagh, 2019).

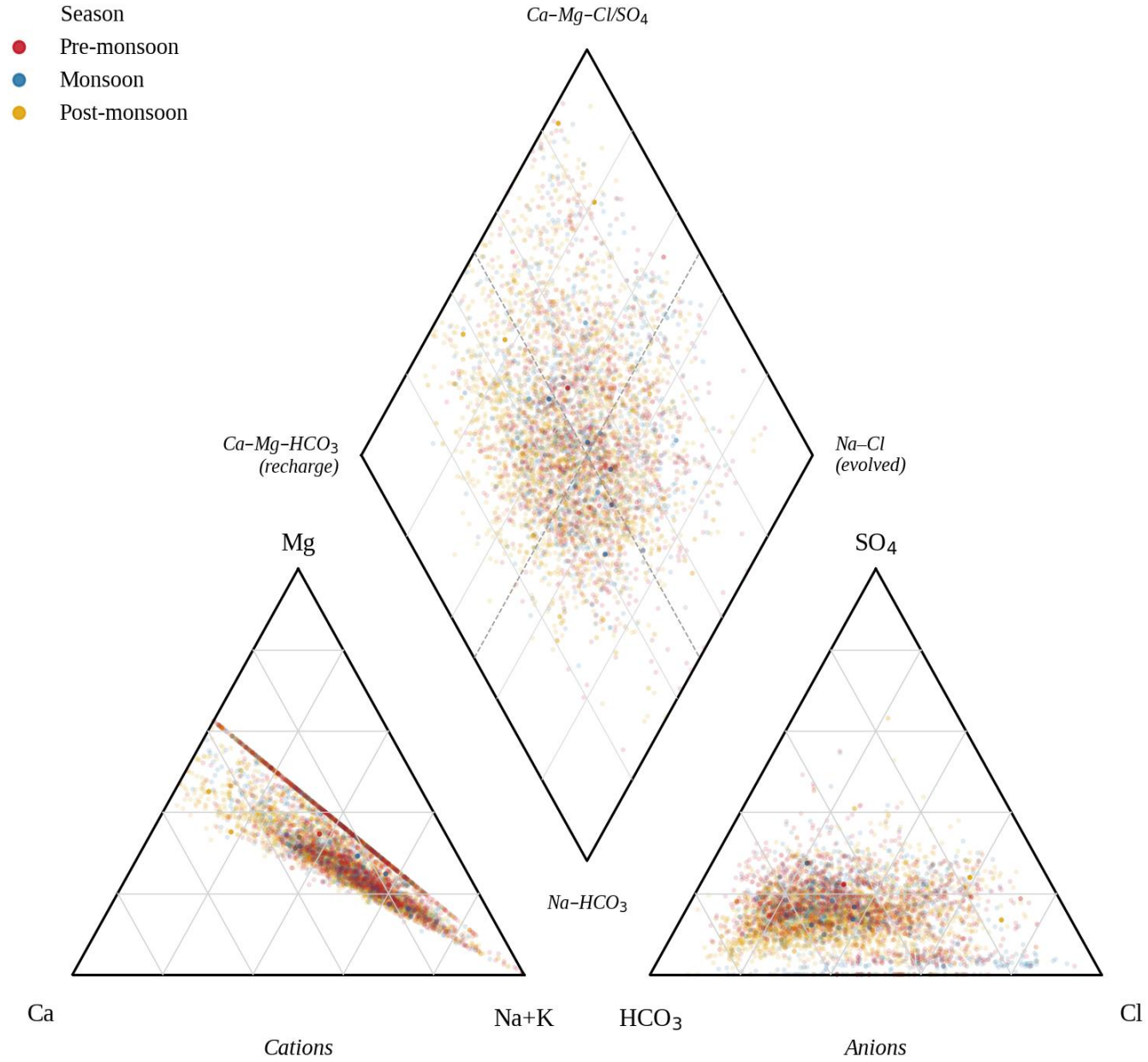

Figure 4. Piper trilinear diagram of Akkalkot groundwater coloured by season. Facies assignment is based on the central diamond, which is independent of the Ca/Mg apportionment used for the cation triangle (Section 3.2).

Table 2. Distribution of hydrochemical facies based on the Piper diamond fields (n = 5,188).

Piper diamond field	Hydrochemical water type	No. of samples	% of total
Alkaline earth (Ca+Mg) + weak acid (HCO3)	Ca–Mg–HCO3 (recharge / fresh)	1696	32.7
Alkaline earth (Ca+Mg) + strong acid (Cl+SO4)	Ca–Mg–Cl/SO4 (reverse exchange)	1374	26.5
Alkali (Na+K) + strong acid (Cl+SO4)	Na–Cl (saline / evolved)	1108	21.4
Alkali (Na+K) + weak acid (HCO3)	Na–HCO3 (base exchange)	1010	19.5

ISSN No. 2321-2705 | DOI: 10.51244/IJRSI |Volume XIII Issue V May 2026

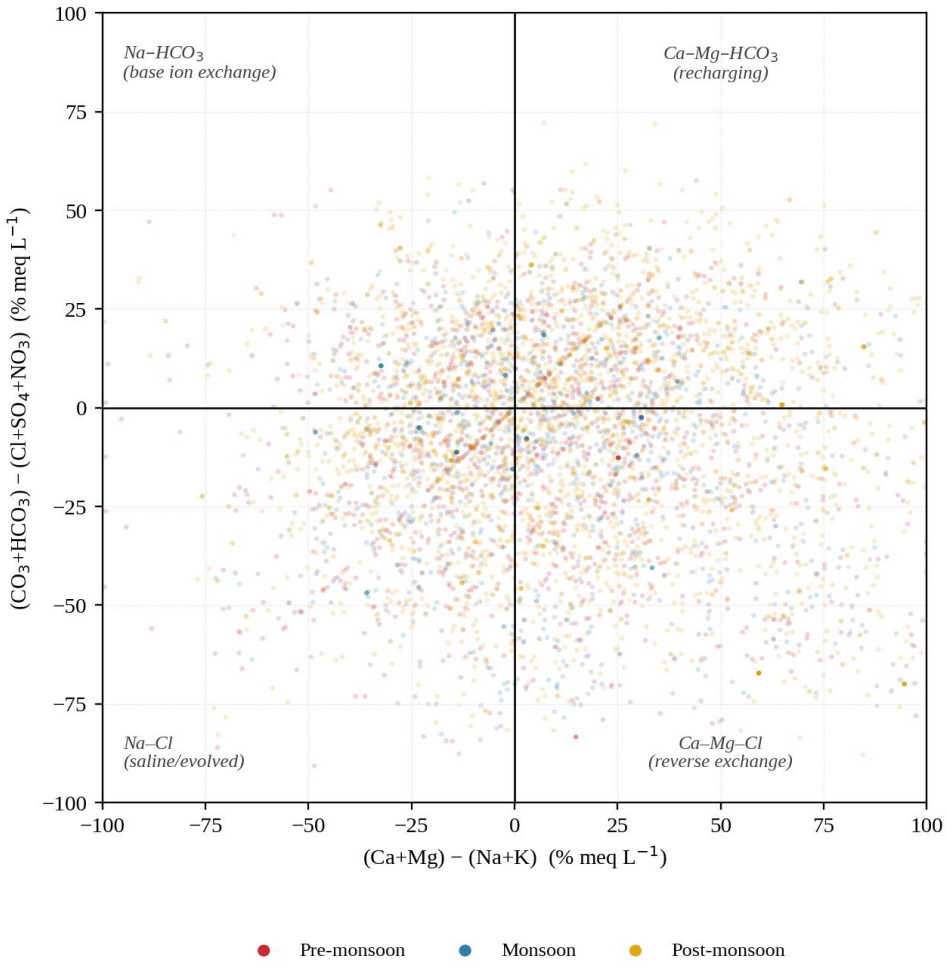

Figure 5. Chadha rectangular diagram showing the geochemical classification of the Akkalkot groundwater and the dominant hydrochemical processes.

Mechanisms controlling groundwater chemistry and water–rock interaction

The Gibbs diagrams (Figure 6) locate the great majority of samples within the rock–water-interaction domain, with the most mineralized waters trending towards the evaporation field and very few approaching the precipitation domain. This confirms that weathering of the aquifer matrix, reinforced by evapoconcentration under the semi-arid climate, is the master control on solute acquisition rather than atmospheric input (R.J. Gibbs, 1970).

The nature of the water–rock interaction is resolved by ionic ratios (Figure 7). The Na^+/Cl^- ratio exceeds unity in 74% of samples (mean 1.7), indicating that sodium is derived chiefly from silicate (plagioclase) weathering and cation exchange rather than from halite dissolution, which would yield a ratio near one (J.D. Hem, 1985). On the $(Ca^{2+} + Mg^{2+})$ versus $(HCO_3^- + SO_4^{2-})$ plot, 64% of samples fall below the 1:1 line, the deficit of alkaline earths relative to these anions again pointing to silicate weathering and to the removal of Ca^{2+} and Mg^{2+} by ion exchange. Schoeller's chloro-alkaline indices are negative in 74% of samples (CAI-I and CAI-II), the diagnostic signature of direct cation exchange in which Ca^{2+} and Mg^{2+} in the groundwater are replaced by Na^+ and K^+ released from clays and weathered basalt (H. Schoeller, 1965; P. Sahu, 2008). This base-exchange softening explains both the sodium enrichment recorded in the facies analysis and the development of the Na–HCO_3 water type.

Collectively, these signatures define the conceptual geochemical evolution illustrated in Figure 2: incongruent dissolution of plagioclase and pyroxene supplies Ca^{2+}, Mg^{2+}, Na^+ and HCO_3^-; cation exchange progressively converts hard Ca–Mg waters to softer Na-rich waters; and evaporative concentration during the long dry season raises overall salinity and chloride. The strong, mutually consistent inter-parameter correlations support this scheme.

ISSN No. 2321-2705 | DOI: 10.51244/IJRSI |Volume XIII Issue V May 2026

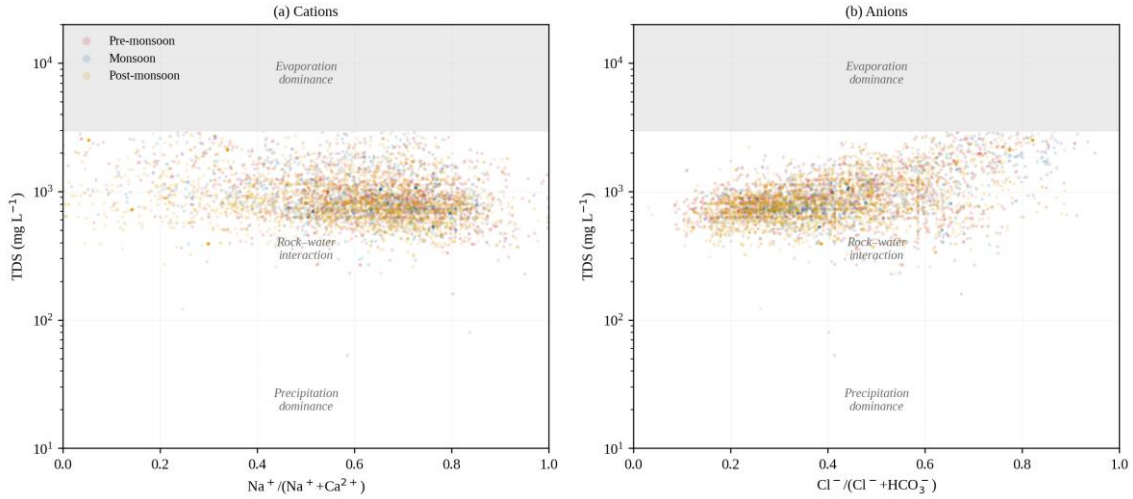

Figure 6. Gibbs diagrams for (a) cations and (b) anions, showing that most Akkalkot groundwater samples plot in the rock–water-interaction field with a trend towards evaporation dominance.

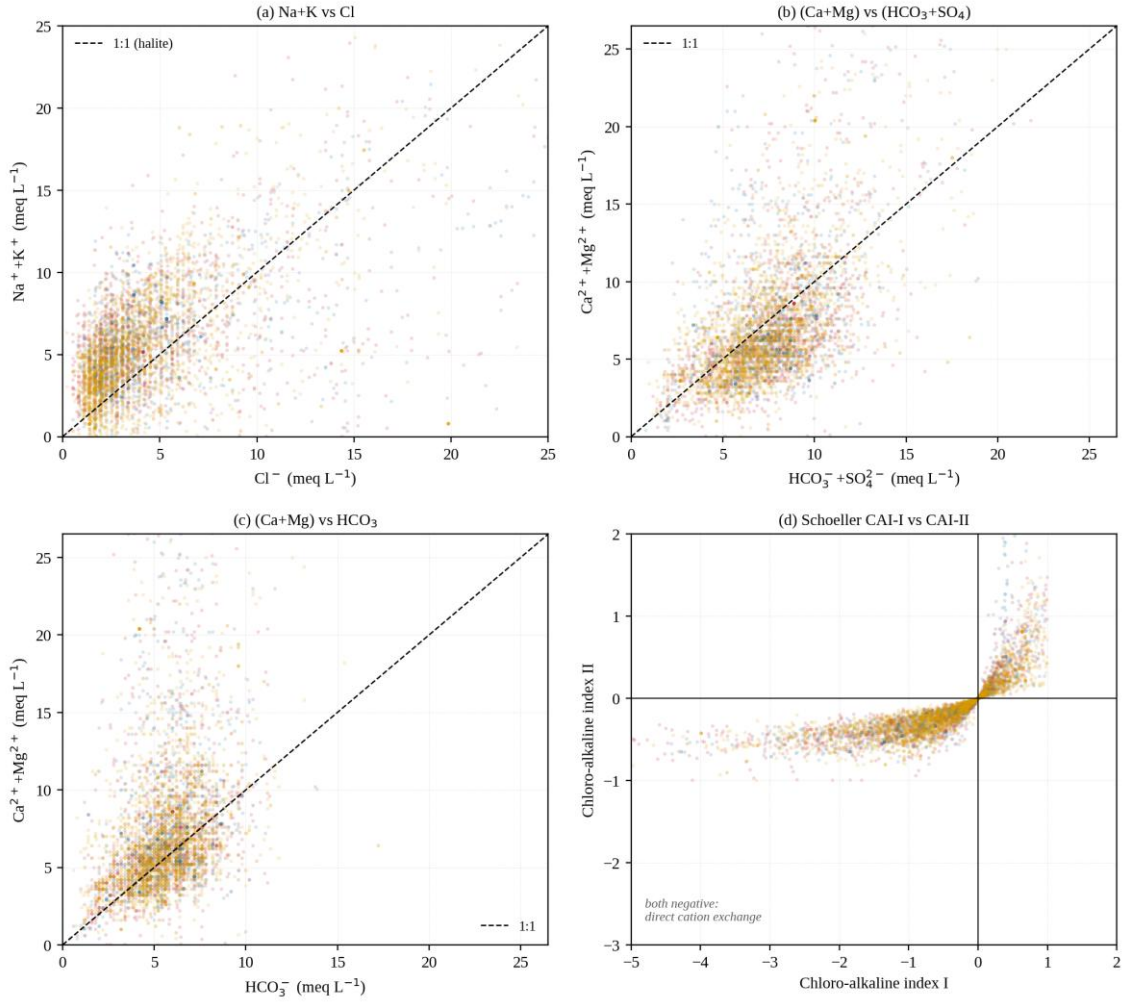

Figure 7. Bivariate plots diagnosing water–rock interaction: (a) $Na^+ + K^+$ vs Cl^-; (b) $(Ca^{2+} + Mg^{2+})$ vs $(HCO_3^- + SO_4^{2-})$; (c) $(Ca^{2+} + Mg^{2+})$ vs HCO_3^-; (d) Schoeller chloro-alkaline indices CAI-I vs CAI-II.

Seasonal and temporal evolution

Seasonal mean concentrations (Table 3, Figure 8) reveal a systematic salinity gradient of pre-monsoon > monsoon > post-monsoon for EC, TDS, chloride and sulphate. The pre-monsoon maximum (mean TDS 1,037 mg L^{-1}; Cl^- 182 mg L^{-1}) reflects evaporative concentration and the longest rock-contact time at the end of the dry season, whereas the post-monsoon minimum (TDS 957 mg L^{-1}; Cl^- 158 mg L^{-1}) records dilution and flushing

ISSN No. 2321-2705 | DOI: 10.51244/IJRSI |Volume XIII Issue V May 2026

by fresh monsoon recharge. Nitrate behaves differently, being marginally higher post-monsoon (mean 58 mg L^{-1}), consistent with the leaching of accumulated fertilizer- and sanitation-derived nitrogen from the soil zone into the aquifer during infiltration (N. Subba Rao, 2006). Bicarbonate and hardness vary only weakly between seasons, as expected for mineral-buffered, weathering-controlled solutes.

Over the eight-year record (Figure 9), mean EC, TDS, hardness, chloride and nitrate show a general downward tendency in the later years (2022–23 and 2023–24 recording the lowest means). Because this is a regulatory surveillance programme rather than a fixed monitoring network, the set of sources sampled differs from year to year; consequently, inter-annual differences in mean concentrations cannot be unambiguously attributed to changes in aquifer chemistry rather than to shifts in sampling coverage. The observed variation is therefore reported here without causal interpretation; a fixed-well network would be required to resolve genuine long-term trends. Across all years the relative ionic proportions, and hence the facies assemblage, remain stable, indicating that the controlling geochemical processes are persistent.

Table 3. Seasonal mean values of selected groundwater quality parameters at Akkalkot.

Parameter	Pre-monsoon	Monsoon	Post-monsoon
pH	7.6	7.5	7.5
EC (µS cm^{-1})	1596.2	1558.3	1486.4
TDS (mg L^{-1})	1036.6	1002.9	957.2
TH (mg L^{-1})	380.1	392.0	373.3
Alkalinity (mg L^{-1})	280.4	284.8	277.6
HCO3 (mg L^{-1})	341.9	347.3	338.5
Cl (mg L^{-1})	182.1	191.4	158.2
SO4 (mg L^{-1})	103.5	96.3	89.2
NO3 (mg L^{-1})	55.2	55.8	57.9
F (mg L^{-1})	0.2	0.2	0.2
SAR	3.8	3.4	3.1
WQI	84.1	82.5	81.1

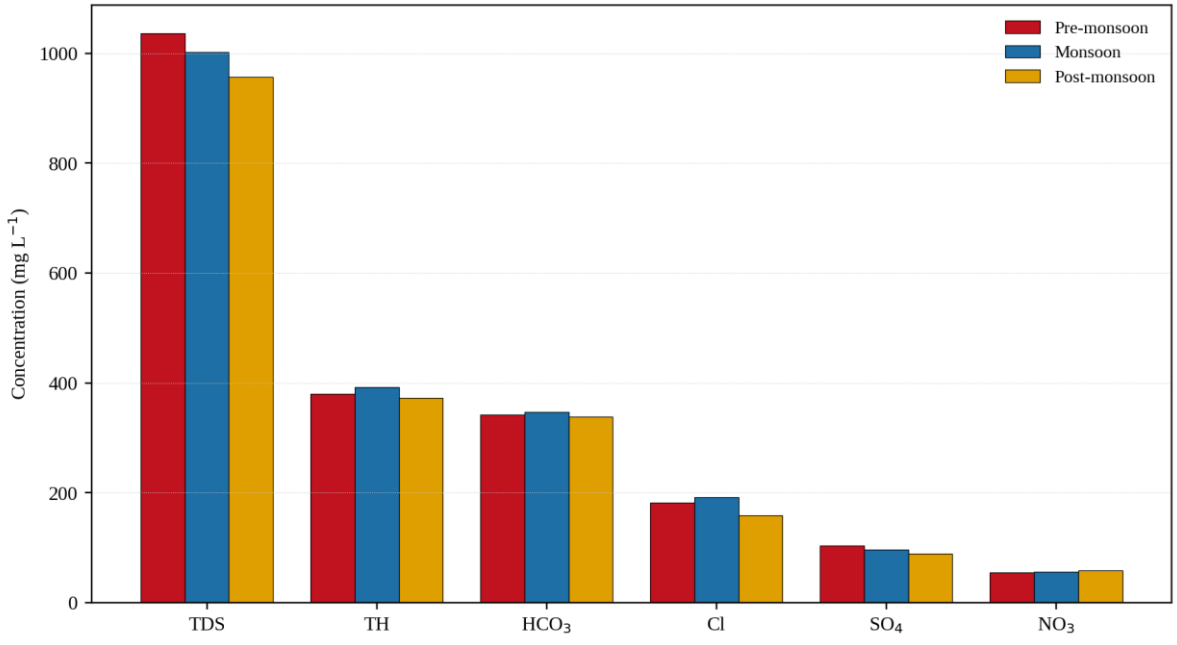

Figure 8. Seasonal variation in mean concentrations of major dissolved constituents in the Akkalkot groundwater.

ISSN No. 2321-2705 | DOI: 10.51244/IJRSI |Volume XIII Issue V May 2026

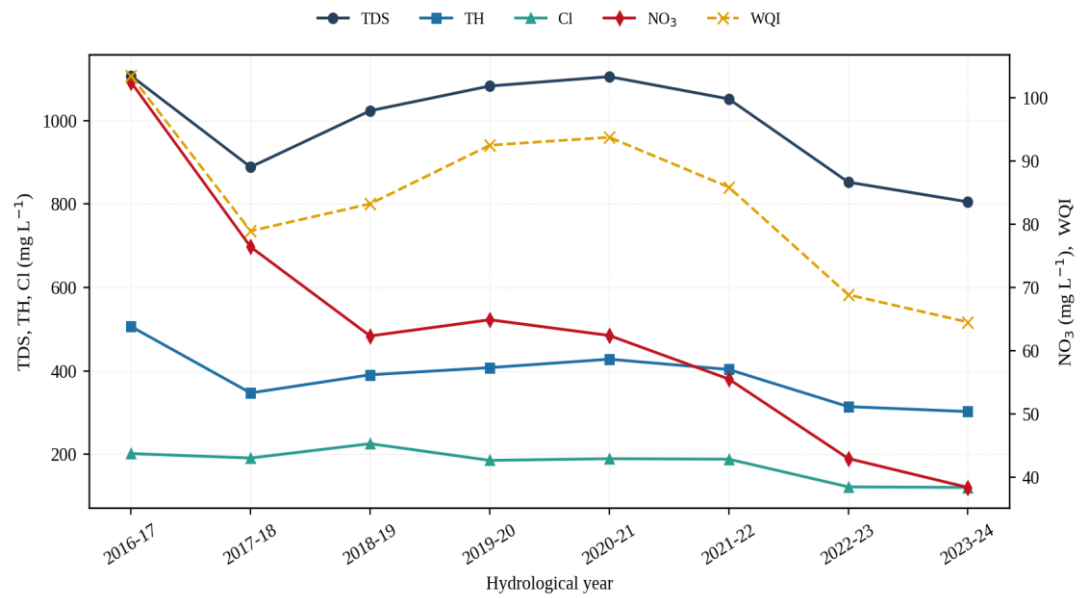

Figure 9. Inter-annual variation (2016–17 to 2023–24) in mean EC, TDS, total hardness, chloride, nitrate and WQI.

Inter-parameter correlations

The Pearson correlation matrix (Figure 10) shows that EC is very strongly correlated with TDS (r = 0.97) and with total hardness (r = 0.90), and strongly with chloride (r = 0.84), sulphate (r = 0.74) and nitrate (r = 0.67), confirming that hardness and chloride salts are the principal contributors to mineralization. The mutual association of Cl^-, SO_4^{2-} and NO_3^- suggests a partly shared anthropogenic and evaporative origin, whereas the weak correlation of pH with all solutes is consistent with carbonate–silicate buffering. Fluoride correlates only moderately with EC (r = 0.43), implying a mineral (rather than salinity) control on its generally low concentrations.

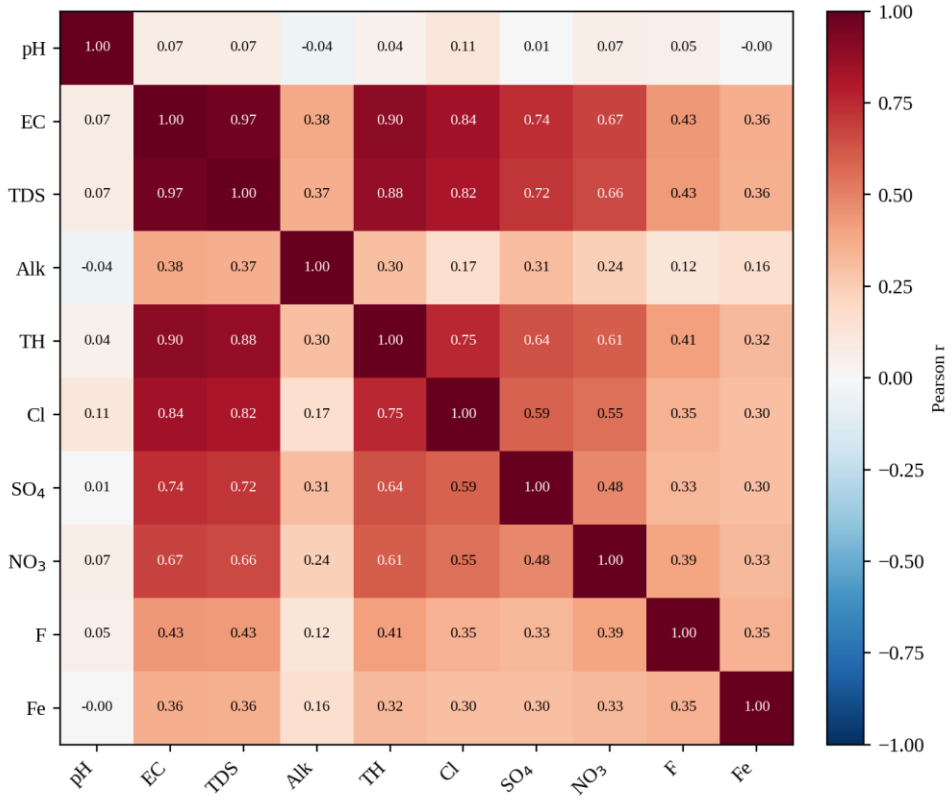

Figure 10. Pearson correlation matrix of the measured groundwater quality parameters.

ISSN No. 2321-2705 | DOI: 10.51244/IJRSI |Volume XIII Issue V May 2026

Drinking-water suitability

Measured against IS 10500:2012 (BIS, 2012), almost all samples are acceptable for pH (only 0.1% lie outside 6.5–8.5), fluoride (0.5% above the acceptable 1.0 mg L^{-1}) and iron (0.4% above 0.3 mg L^{-1}). The principal exceedances (Figure 11) are for total hardness (83% above the acceptable 200 mg L^{-1}; 11% above the permissible 600 mg L^{-1}), TDS (94% above 500 mg L^{-1} but only 5% above the permissible 2,000 mg L^{-1}) and alkalinity (80% above 200 mg L^{-1}). Critically, nitrate exceeds the 45 mg L^{-1} limit—for which no relaxation is permitted—in 29% of samples, the most serious health concern because elevated nitrate is associated with infant methaemoglobinaemia (WHO, 2017). The anthropogenic origin is clear, but the relative contributions of agricultural fertilizers and on-site sanitation cannot be separated from the present dataset; isotopic analysis ($\delta^{15}N$–NO_3^-) or a spatially referenced land-use map overlaid on nitrate exceedance locations would allow these two pathways to be distinguished in future work. High hardness, while not directly hazardous to health, causes scaling, soap wastage and palatability problems.

These individual criteria are integrated by the water quality index (Table 4, Figure 12). The mean WQI is 82 (median 70), and 78% of samples fall in the excellent (12%) or good (67%) categories, 19% are poor, and 2.3% are very poor to unsuitable. Source-wise, handpump waters carry the highest mean salinity, hardness, nitrate and WQI, and dug-well waters the lowest (Table 5), reflecting deeper or longer-residence circulation tapped by handpumps versus the more rapidly recharged, dilute shallow water of dug wells. Overall, the groundwater is potable in most of the taluka but requires attention to hardness and salinity, and active management of nitrate, before unrestricted drinking use; point-of-use softening or blending, and protection of sources from sanitation and agricultural contamination, are advisable in the affected pockets.

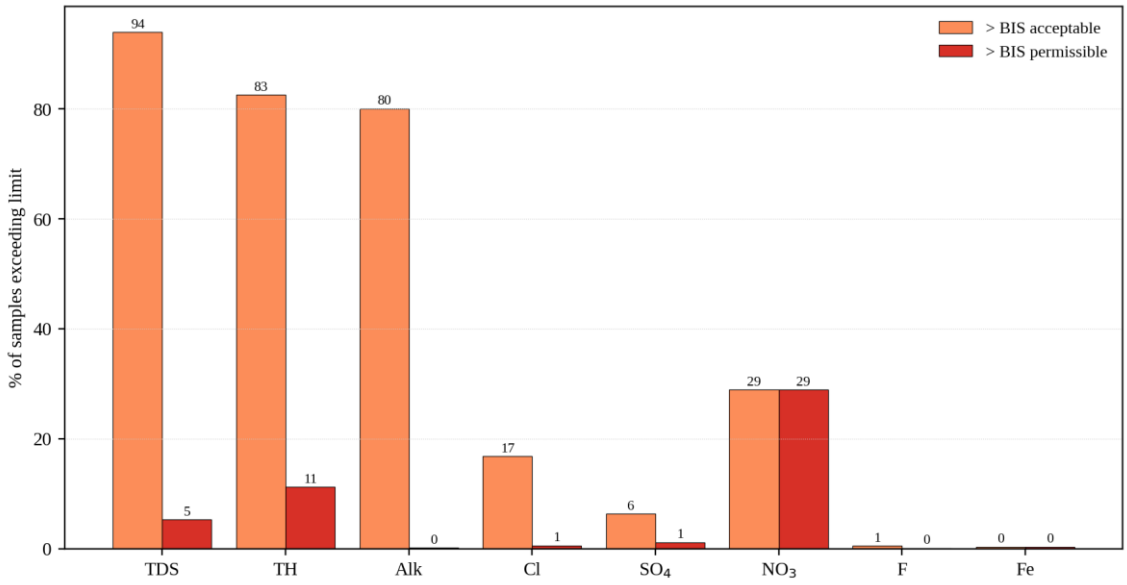

Figure 11. Percentage of groundwater samples exceeding the BIS (2012) acceptable and permissible limits for major parameters.

Table 4. Water quality index (WQI) classification of the Akkalkot groundwater.

WQI range	Water quality class	No. of samples	% of samples
<50	Excellent	626	11.7
50-100	Good	3570	66.7
100-200	Poor	1035	19.3
200-300	Very poor	110	2.1
>300	Unsuitable	11	0.2

ISSN No. 2321-2705 | DOI: 10.51244/IJRSI |Volume XIII Issue V May 2026

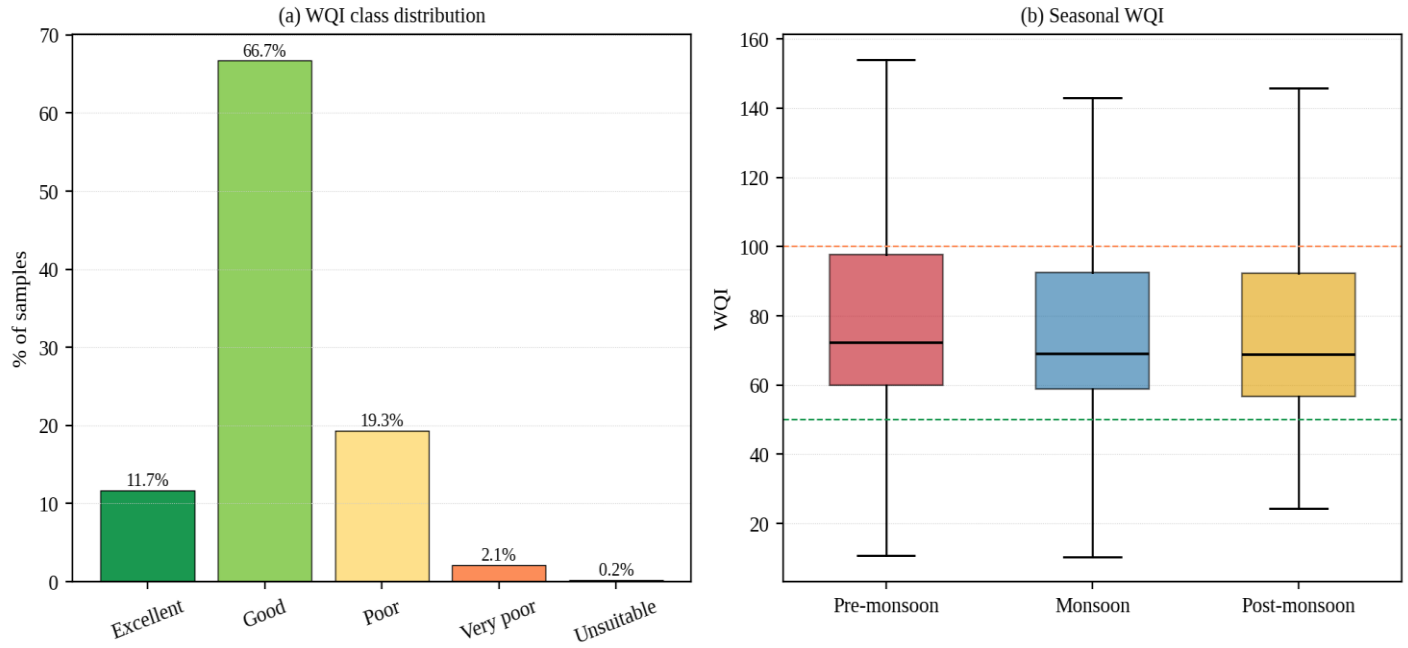

Figure 12. Water quality index of the Akkalkot groundwater: (a) distribution of samples among WQI classes; (b) seasonal variation of WQI.

Table 5. Source-wise mean values of selected parameters and WQI (units: EC in µS cm⁻¹; others in mg L⁻¹).

Source type	n	EC	TDS	TH	Cl	NO3	Mean WQI
Handpump	2254	1674.3	1079.3	425.1	194.9	63.7	89.5
Dug well	1605	1337.5	859.5	328.0	133.6	48.0	71.9
Borewell	1488	1525.6	990.4	365.4	178.0	55.6	82.5

Irrigation-water suitability

Because groundwater is also the chief irrigation source, its agricultural quality was evaluated (Table 6). The sodium adsorption ratio is low (mean 3.4) and below 10 in 99% of samples, so the sodium (alkali) hazard to soil structure is minimal; on the US Salinity Laboratory diagram (Figure 13) the samples plot overwhelmingly in the low-sodium classes (S1) but spread across medium-to-very-high salinity classes (C2–C4), confirming that salinity, not sodicity, is the dominant irrigation constraint (L.A. Richards, 1954). Sodium percentage is mostly permissible (42%) to good (27%), with 17% in the doubtful range; residual sodium carbonate is safe (<1.25 meq L⁻¹) in 83% of samples; Kelley's ratio is below one in 60%; and the permeability index places 95% of samples in Classes I–II (L.D. Doneen, 1964). The groundwater is therefore generally suitable for irrigation of salt-tolerant crops with adequate drainage, although the more saline pre-monsoon waters warrant caution.

Table 6. Irrigation water quality indices for the Akkalkot groundwater.

Index	Reference	Range / class	% of samples	Mean (min–max)
SAR	L.A. Richards, 1954	<10 (Excellent)	98.6	3.36 (-3.77–80.7)
Na %	L.V. Wilcox, 1955	40–60 (Permissible)	42.1	43.5 (0.0–99.7)
RSC (meq L⁻¹)	F.M. Eaton, 1950	<1.25 (Safe)	83.1	-1.99 (-47.68–10.83)
Kelly ratio	W.P. Kelley, 1940	<1 (Suitable)	60.4	1.34 (0.0–368.49)
Permeability index (%)	L.D. Doneen, 1964	>75 (Class I)	29.5	63.4 (3.1–134.6)

ISSN No. 2321-2705 | DOI: 10.51244/IJRSI |Volume XIII Issue V May 2026

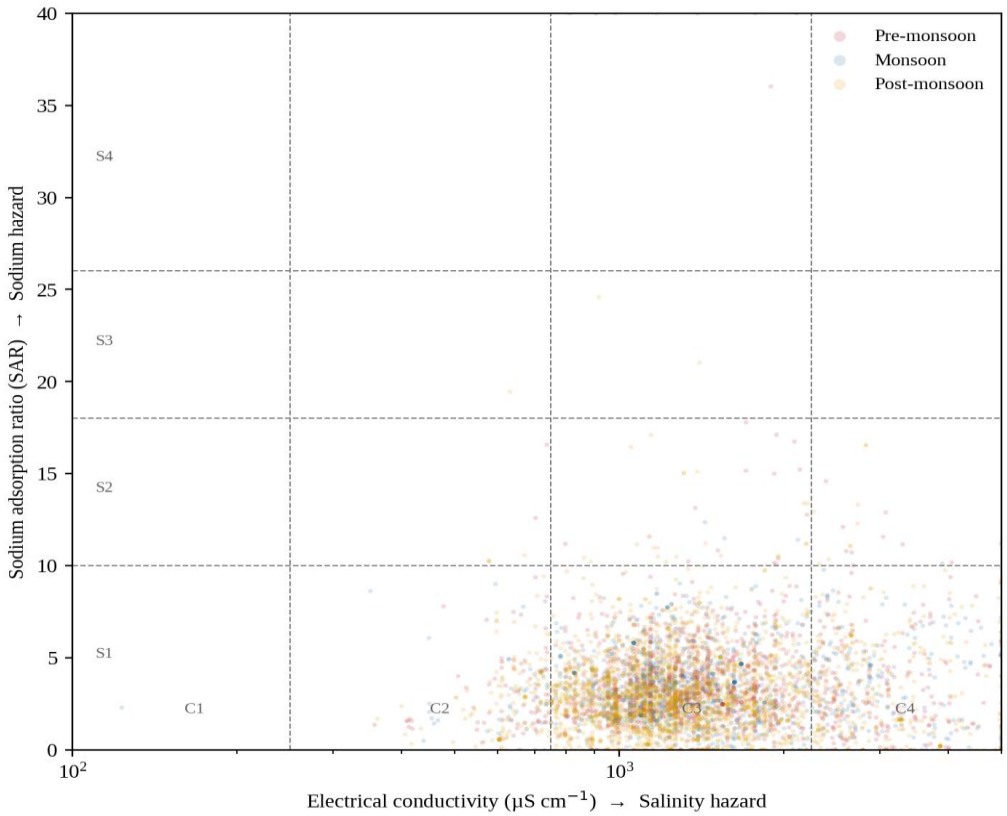

Figure 13. US Salinity Laboratory (USSL) diagram for irrigation-water classification of the Akkalkot groundwater (SAR vs electrical conductivity).

CONCLUSIONS

Groundwater in the semi-arid Deccan basaltic terrain of Akkalkot taluka is neutral to slightly alkaline, moderately mineralized and predominantly hard to very hard, with bicarbonate and alkaline earths as the leading ions. Piper and Chadha diagrams identify a mixed facies assemblage led by Ca–Mg–HCO_3 recharge water that evolves through Na–HCO_3 to Na–Cl types, recording a clear hydrogeochemical evolution along the flow path. Gibbs plots, Na^+/Cl^- ratios and consistently negative chloro-alkaline indices establish silicate (plagioclase) weathering and direct cation exchange, modified by evapoconcentration, as the dominant controls on water chemistry—the expected fingerprint of a basaltic aquifer. Chemistry varies seasonally, with maximum salinity in the pre-monsoon and dilution after the monsoon, while inter-annual variation is modest and the facies pattern stable. Judged against BIS and WHO norms, the water is potable across most of the taluka (78% excellent–good on the WQI), but high hardness, salinity and—most importantly—nitrate (exceeding the limit in 29% of samples) constrain its drinking suitability. For irrigation the principal limitation is salinity rather than sodicity. Periodic monitoring, nitrate-source control, source protection and point-of-use treatment in the affected pockets are recommended to safeguard this vital resource.

ACKNOWLEDGEMENTS

The author expresses sincere gratitude to the Hon. Commissioner, Groundwater Surveys and Development Agency (GSDA), for providing the necessary institutional support, facilities, and encouragement to carry out this research work successfully. The author is also deeply thankful to the Hon. Deputy Director, Groundwater Surveys and Development Agency (GSDA), Pune Region, for valuable guidance, administrative support, and for facilitating the resources required for the completion of this study. Their constant encouragement and support have been instrumental in accomplishing this research.

The author further acknowledges the support extended by the officers and staff of District Groundwater Surveys and Development Agency, Solapur for their cooperation, technical assistance, and data support during the course of this research work.

REFERENCES

1. A.M. Piper (1944), A graphic procedure in the geochemical interpretation of water analyses, Transactions of the American Geophysical Union, Vol.25, No.6, pp.914–928.
2. APHA (2017), Standard Methods for the Examination of Water and Wastewater, 23rd ed., American Public Health Association, Washington DC.
3. BIS (2012), IS 10500:2012 Indian Standard Drinking Water – Specification (Second Revision), Bureau of Indian Standards, New Delhi, pp.1–11.
4. C.N. Sawyer, P.L. McCarty (1967), Chemistry for Sanitary Engineers, 2nd ed., McGraw-Hill, New York, pp.1–518.
5. CGWB (2013), Ground Water Information, Solapur District, Maharashtra, Central Ground Water Board, Ministry of Water Resources, Government of India, pp.1–22.
6. D. Marghade, D.B. Malpe, A.B. Zade (2012), Major ion chemistry of shallow groundwater of a fast growing city of Central India, Environmental Monitoring and Assessment, Vol.184, No.4, pp.2405–2418.
7. D.B. Panaskar, V.M. Wagh, A.A. Muley, S.V. Mukate, et al. (2016), Evaluating groundwater suitability for the domestic, irrigation and industrial purposes in Nanded Tehsil, Maharashtra, India, Modeling Earth Systems and Environment, Vol.2, No.74, pp.1–13.
8. D.K. Chadha (1999), A proposed new diagram for geochemical classification of natural waters and interpretation of chemical data, Hydrogeology Journal, Vol.7, No.5, pp.431–439.
9. F. Birajdar and M. Shaikh, "Groundwater exploration and assessment in arid and semi-arid regions of basaltic terrain of Solapur: Lessons learned and future prospects," Int. J. Innov. Sci. Res. Technol., pp. 2763-2776, 2024d, doi: 10.38124/ijisrt/IJISRT24APR2344.
10. F.M. Eaton (1950), Significance of carbonates in irrigation waters, Soil Science, Vol.69, No.2, pp.123–133.
11. H. Schoeller (1965), Qualitative evaluation of groundwater resources, in: Methods and Techniques of Groundwater Investigation and Development, UNESCO, Paris, pp.54–83.
12. J.D. Hem (1985), Study and Interpretation of the Chemical Characteristics of Natural Water, 3rd ed., U.S. Geological Survey Water-Supply Paper 2254, pp.1–263.
13. K.R. Karanth (1987), Ground Water Assessment, Development and Management, Tata McGraw-Hill, New Delhi, pp.1–720.
14. L.A. Richards (1954), Diagnosis and Improvement of Saline and Alkali Soils, USDA Agriculture Handbook No.60, U.S. Department of Agriculture, Washington DC, pp.1–160.
15. L.D. Doneen (1964), Notes on Water Quality in Agriculture, Water Science and Engineering Paper 4001, Department of Water Science and Engineering, University of California, Davis.
16. L.V. Wilcox (1955), Classification and Use of Irrigation Waters, USDA Circular No.969, U.S. Department of Agriculture, Washington DC, pp.1–19.
17. M. Shaikh and F. Birajdar, "Ensuring purity and health: A comprehensive study of water quality testing labs in Solapur district for community well-being," Int. J. Innov. Sci. Res. Technol., vol. 9, no. 1, pp. 271-281, 2024b, doi: 10.5281/zenodo.10622956.
18. M. Shaikh and F. Birajdar, "Groundwater and ecosystems: Understanding the critical interplay for sustainability and conservation," EPRA Int. J. Multidiscip. Res., vol. 10, no. 3, pp. 181-186, 2024, doi: 10.36713/epra16111.
19. M. Shaikh and F. Birajdar, "Groundwater and public health: Exploring the connections and challenges," Int. J. Innov. Sci. Res. Technol., vol. 9, no. 2, pp. 1351-1361, 2024a, doi: 10.5281/zenodo.10730864.
20. M. Shaikh and F. Birajdar, "Mapping of feasibility of groundwater for drinking water zones of Akkalkot taluk, Solapur, India using GIS techniques," Int. J. Sci. Res., vol. 4, no. 4, pp. 1709-1713, 2015, doi: 10.21275/15041507.
21. M. Vasanthavigar, K. Srinivasamoorthy, K. Vijayaragavan, et al. (2010), Application of water quality index for groundwater quality assessment: Thirumanimuttar sub-basin, Tamilnadu, India, Environmental Monitoring and Assessment, Vol.171, No.1–4, pp.595–609.
22. N. Adimalla, S. Venkatayogi (2018), Geochemical characterization and evaluation of groundwater suitability for domestic and agricultural utility in semi-arid region of Basara, Telangana State, South India, Applied Water Science, Vol.8, No.44, pp.1–14.

ISSN No. 2321-2705 | DOI: 10.51244/IJRSI |Volume XIII Issue V May 2026

23. N. Subba Rao (2006), Seasonal variation of groundwater quality in a part of Guntur District, Andhra Pradesh, India, Environmental Geology, Vol.49, No.3, pp.413–429.
24. N.J. Pawar, G.M. Pondhe, S.F. Patil (1998), Groundwater pollution due to sugar-mill effluent, at Sonai, Maharashtra, India, Environmental Geology, Vol.34, No.2–3, pp.151–158.
25. P. Sahu, P.K. Sikdar (2008), Hydrochemical framework of the aquifer in and around East Kolkata Wetlands, West Bengal, India, Environmental Geology, Vol.55, No.4, pp.823–835.
26. P.K. Naik, A.K. Awasthi (2003), Groundwater resources assessment of the Koyna River basin, India, Hydrogeology Journal, Vol.11, No.5, pp.582–594.
27. R.J. Gibbs (1970), Mechanisms controlling world water chemistry, Science, Vol.170, No.3962, pp.1088–1090.
28. V.M. Wagh, D.B. Panaskar, S.V. Mukate, A.A. Muley, et al. (2019), Health risk assessment of heavy metal contamination in groundwater of Kadava River basin, Nashik, India, Modeling Earth Systems and Environment, Vol.5, No.4, pp.1–12.
29. W.P. Kelley (1940), Permissible composition and concentration of irrigation waters, Proceedings of the American Society of Civil Engineers, Vol.66, pp.607–613.
30. WHO (2017), Guidelines for Drinking-water Quality, 4th ed. incorporating the first addendum, World Health Organization, Geneva, pp.1–541.

ISSN No. 2321-2705 | DOI: 10.51244/IJRSI |Volume XIII Issue V May 2026

APPENDIX

APPENDIX A. Ca/Mg Apportionment Method, Uncertainty Assessment and Sensitivity Analysis

A.1 Rationale for the TDS-dependent Ca/Mg splitting function. Because the routine surveillance dataset does not include individually measured Ca^{2+} and Mg^{2+}, their partition from total hardness (expressed as $CaCO_3$) was performed using a TDS-dependent molar Ca/Mg ratio derived from paired Ca/Mg measurements in the Deccan basalt literature (N.J. Pawar, 1998; M.A. Shaikh, 2024). In freshly recharged, dilute waters (TDS < 300 mg L^{-1}) the molar Ca/Mg ratio is approximately 1.7, reflecting preferential dissolution of Ca-rich plagioclase (labradorite–andesine). With increasing residence time and salinity, calcite precipitation selectively removes Ca^{2+} while Mg^{2+} remains in solution, reducing the ratio to approximately 0.7 at TDS > 1,500 mg L^{-1}. A linear interpolation between these end-members was applied on a sample-by-sample basis. This approach is used solely for positioning points on the Piper cation triangle; the facies assignment is based on the central Piper diamond and the Chadha diagram, both of which depend only on the (Ca^{2+} + Mg^{2+}) sum and are therefore independent of the Ca/Mg split (as noted in Section 3.2).

A.2 Sensitivity of Piper cation-triangle positions. To bound the uncertainty introduced by the Ca/Mg assumption, the Piper diagram was constructed under two extreme scenarios: (i) a fixed Ca/Mg ratio of 1.7 applied to all samples, and (ii) a fixed ratio of 0.7 applied to all samples. Under scenario (i) samples plot somewhat closer to the Ca apex; under scenario (ii) they shift towards Mg. In both cases, the central diamond classification—and therefore all facies percentages reported in Table 2—is unchanged, confirming that the uncertainty in Ca/Mg partitioning does not affect the study's conclusions. [Note to authors: the two sensitivity Piper plots should be added as Figure A1 in the final manuscript.]

A.3 Supplementary table: range of derived ionic concentrations and charge-balance uncertainty. The table below summarises the calculated Ca^{2+}, Mg^{2+} and Na^{+}+K^{+} values alongside an estimate of the charge-balance error (CBE = [(Σcations − Σanions)/(Σcations + Σanions)] × 100). Because Na^{+}+K^{+} is derived by charge-balance closure, the CBE for these samples reflects uncertainty in the measured anion and hardness values rather than an independent analytical check. Samples with a negative Na^{+}+K^{+} residual (CBE < −5%, n = 166, 3.1% of total) were excluded from facies classification, as noted in Section 3.2.

Table A1. Descriptive statistics of derived ionic concentrations and charge-balance error (n = 5,352; units mg L^{-1} except CBE in %).

Parameter	Min	Max	Mean	SD	Notes
Ca^{2+} (mg L^{-1})*	0.24	560.67	75.97	51.18	TDS-dependent Ca/Mg split (r ≈ 1.7–0.7)
Mg^{2+} (mg L^{-1})*	0.15	339.93	46.06	31.03	TDS-dependent Ca/Mg split (r ≈ 1.7–0.7)
Na^{+}+K^{+} raw (mg L^{-1})*	−311.5	796.79	132.23	94.64	Full dataset (n = 5,352); includes 166 excluded samples with negative residual
Na^{+}+K^{+} valid (mg L^{-1})*	0	796.79	140.6	86.2	Facies-classified subset (n = 5,186); negative residuals excluded
CBE (%) — valid samples	≈ 0	≈ 0	0	0	CBE = 0 by construction (Na^{+}+K^{+} derived to close charge balance); n = 5,186
CBE (%) — excluded samples	−47	−6	—	—	Physically implausible (anion sum exceeds cation sum); excluded from facies classification (n = 166, 3.1%)

* Derived parameter (not directly measured). Ca^{2+} and Mg^{2+} apportioned from total hardness using TDS-dependent molar Ca/Mg ratio (see A.1); Na^{+}+K^{+} estimated by ionic charge-balance closure (see Section 3.2). Min/Max values listed under 'Min' and 'Max' columns for Na^{+}+K^{+} raw correspond to the extremes of the full dataset before exclusion of negative residuals. The mean and SD for Na^{+}+K^{+} valid (n = 5,186) are estimated after removing the 166 excluded samples. CBE range for excluded samples is estimated assuming mean Ca^{+}+Mg^{2+} ionic strength; actual values depend on the hardness and anion loads of individual excluded samples.